New Journal of Physics
The open–access journal for physics

Tectonic microplates in a wax model of sea-floor spreading

Richard F Katz[1], **Rolf Ragnarsson**[2] **and Eberhard Bodenschatz**[2,3]

[1] Lamont-Doherty Earth Observatory of Columbia University, Palisades, NY, USA
[2] Laboratory of Atomic and Solid State Physics, Cornell University, Ithaca, NY, USA
[3] Max Planck Institute for Dynamics and Self-Organization, Göttingen, Germany
E-mail: katz@ldeo.columbia.edu

New Journal of Physics **7** (2005) 37
Received 21 November 2004
Published 1 February 2005
Online at http://www.njp.org/
doi:10.1088/1367-2630/7/1/037

Abstract. Rotating, growing microplates are observed in a wax analogue model of sea-floor spreading. Wax microplates are kinematically similar to sea-floor tectonic microplates in terms of spreading rate and growth rate. Furthermore, their spiral pseudofault geometry is quantitatively consistent with Schouten's oceanic microplate model. These results suggest that Schouten's edge-driven microplate model captures the kinematics of tectonic microplate evolution on Earth. Based on the wax observations, a theory for the nucleation of overlapping spreading centres, the precursors of tectonic microplates, is developed.

PII: S1367-2630(05)89897-0

Contents

1. Introduction

Sea-floor microplates are small areas of rigidly rotating lithosphere located along divergent tectonic plate boundaries called mid-ocean ridges. They are among the most exotic and enigmatic of tectonic morphologies. The mechanics of their formation, and of mid-ocean ridge segmentation in general, is not well understood. This is due, in part, to the inaccessiblity of the ocean floor to direct observation and to the fact that microplate evolution takes place over millions of years. We describe a modern version of classic laboratory-scale wax analogue experiments [1, 2] that permits detailed observations and quantitative measurement of rotating, growing microplates [3] (see the movie, field width 6 mm).

While there has been skepticism regarding the scalability of wax models, we find that wax analogue models provide a useful means for studying the tectonics of plate spreading. In figure 1 we show that wax microplates obey the same quantitative relation between spreading rate, growth rate and spiral pseudofault geometry as their oceanic cousins. Our wax-to-Earth scaling relations [4] indicate that the dimensions of wax microplates are consistent with estimates for oceanic microplates [5, 6]. Through close observation (e.g. figure 4), we have developed a theory for the nucleation of overlapping spreading centres (OSCs), known to be the precursors of microplates in wax and on Earth.

Microplates were discovered on the ocean floor in the early 1970s through surveys of their magnetic anomalies, seismicity and topography [7]–[9]. An explanation of their peculiar geometry and possible modes of formation were proposed shortly afterwards [10]. During the 1980s microplates were recognized as an important tectonic feature of mid-ocean ridges, particularly the East Pacific Rise (EPR) [11, 12] and much work was done to comprehensively map their structure (e.g. [13]). At least 12 paleo- and active microplates are known to exist in the Pacific basin and additional ones are suspected to exist based on patterns observed in altimetry data [32]. The Easter microplate, shown in figure 3(c), sits on the EPR near 25°S between the Pacific and Nazca plates. High-resolution maps enabled the development of kinematic models [6, 14] but due to the difficulty of interpreting sea-floor data, these models have not been conclusively verified. Furthermore, important questions regarding the origin of microplates and

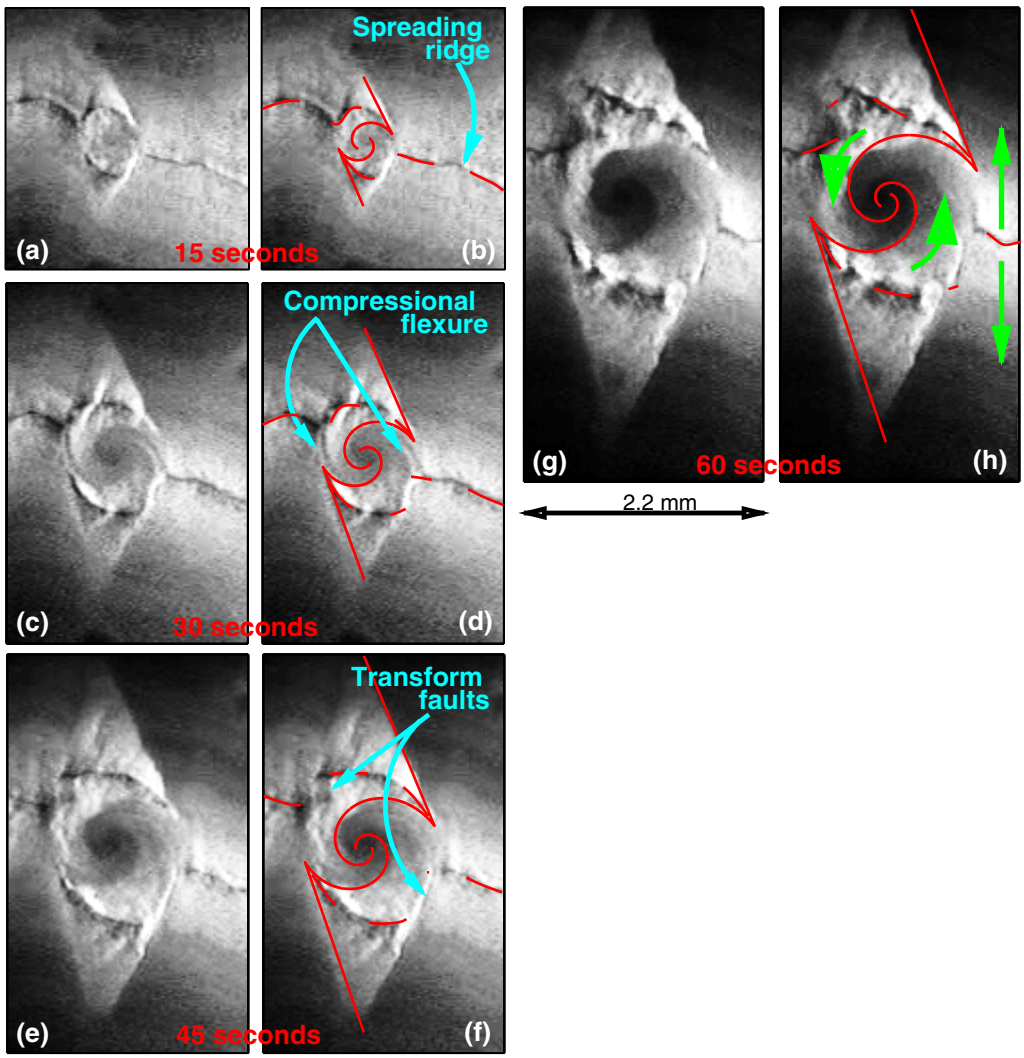

Figure 1. Time series of images showing a growing microplate at 15 second intervals. Spreading is to the top and bottom of each image at a half-rate of 35 μm s^{-1}. **Left column**, images of the microplate. **Right column**, images identical to those in the left column but with pseudofault pairs and spreading ridge traces overlayed in red. The inner pseudofaults were generated using equations (A.6) and (A.7). Measurements of the outer pseudofaults input into the model are $\alpha_{top} = 23^\circ$, $\phi^f_{top} = 18^\circ$, $\alpha_{bottom} = 18^\circ$, $\phi^f_{bottom} = 13^\circ$. Ridge traces were drawn by hand. Blue annotations indicate morphological features. Green arrows show the direction of motion of the main plates and the direction of microplate rotation.

their eventual death have not been answered. For example, there are disagreements about the extent to which external factors such as magma supply [15] or changes in plate motion [16, 17] affect these processes. Current numerical simulations cannot reproduce the coupled fluid–solid deformation processes responsible for microplate nucleation and growth at mid-ocean ridges. On the other hand, published results from a wax analogue model yielded the first observations of OSCs, morphological precursors to microplates, before their discovery on the sea-floor [1].

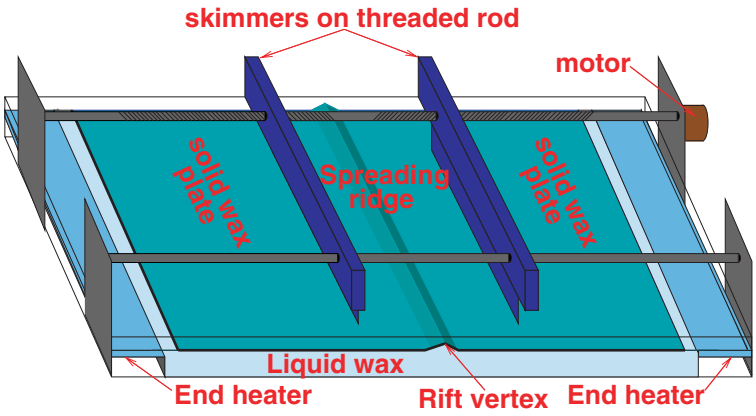

Figure 2. Schematic diagram of the experimental setup. A rectangular tank of size $114 \times 36 \times 10\,\mathrm{cm}^3$ is filled with Shell Callista 158 wax which melts at about 72 °C [20, 34]. The mechanical properties of micro-crystalline wax are brittle at room temperature and paste-like close to the melting point. No detailed mechanical measurements are performed. The tank is heated from below to (80.0 ± 0.05) °C and cooled from above by a constant flow of air at (12.0 ± 2.0) °C. The weakly turbulent refrigerated air flow is directed vertically downwards. Before each run, the wax is brought to temperature equilibrium at which a layer of solid wax is present on the surface. Skimmers embedded in the solid wax are attached to a threaded rod that is driven by a micro-stepping motor. A detailed description of this setup has been previously published [21]. The rift is initiated with a straight cut through the wax, perpendicular to the spreading direction. Divergence at this cut causes liquid wax to rise into the rift and solidify. Illumination from below permits us to image the plate thickness at the rift from above using a video camera. As the wax plate thickens, it scatters more of the transmitted light and appears darker. In images of wax microplates shown here, spreading is towards the top and bottom of the image and the rift appears as a dark line.

We demonstrate that wax models still possess significant potential to provide insight into this long-standing problem.

2. Experiments

Our experimental setup is shown in figure 2. Three distinct morphological regimes exist for ranges in spreading rate of an initially orthogonal rift. At slow half-spreading rates ($\sim$10–30 $\mu\mathrm{m\,s}^{-1}$) the straight rift is stable and forms a topographic low. At moderate rates ($\sim$30–60 $\mu\mathrm{m\,s}^{-1}$) the straight rift becomes unstable and OSCs and microplates form, evolve and die on the ridge. In this regime, the ridge has little or no relief. At higher half-spreading rates still, the microplates lose their internal rigidity and become, in an intermediate stage, fault gouge zones and finally ($\gtrsim$70 $\mu\mathrm{m\,s}^{-1}$) transform faults at a ridge that forms a topographic high. Here, we focus on the microplate regime but stress that because of our simple initial condition (a straight cut orthogonal to the direction of spreading) we do not expect these velocity regimes to correspond to various

mid-ocean ridges on Earth. Variation of rift profile with spreading rate [18] and the evolution of transform faults [3] have both been studied using this experimental apparatus. A similar experiment has been used to study lineaments on Europa [19].

2.1. Scaling

While we have not demonstrated dynamical scaling (the dynamics of microplate evolution are not well constrained [22]) we contend that geometric similarities between our model and Earth's mid-ocean ridges are significant. To interpret our results we must consider how experimental distance and time scale to the Earth. A time scaling can be determined by comparing rotation rates: a mature oceanic microplate rotates 20° in about 1 Ma while a wax microplate completes this rotation in about 5 seconds. To determine length and velocity scalings we consider the thermal process of lithospheric thickening. This process is modelled by considering the instantaneous cooling of a semi-infinite half-space,

$$L = 2\alpha\sqrt{\kappa t}, \tag{1}$$

where L is the thickness of the lithosphere, α is a constant that depends on the thermal details of the phase boundary, κ is the thermal diffusivity and t is time [23]. A scaling for horizontal length, x, is then given by [4]

$$\frac{x_w}{x_e} = \gamma \left(\frac{t_w}{t_e}\right)^{1/2}, \tag{2}$$

where the subscript w signifies wax and e signifies Earth. The thermal scaling parameter, $\gamma = \frac{\alpha_w}{\alpha_e}(\frac{\kappa_w}{\kappa_e})^{1/2} \approx 0.05$ is determined by fitting equation (1) to measurements of wax thickness at distances away from the rift to obtain $\alpha_w\sqrt{\kappa_w}$. Applying equation (2), we find that 1 mm in the wax experiment scales to about 50 km on Earth. Since a typical wax microplate reaches several mm in diameter, this scaling is consistent with published dimensions of oceanic microplates [5, 6].

3. Analysis

Our analysis of wax microplate morphology employs a kinematic model of microplate evolution proposed and applied to the Easter microplate by Schouten *et al* [6]. The Schouten model states that the rigid motion of a microplate is like that of a ball rotating between two parallel, moving plates. Unlike the ball, however, a microplate grows by accreting young lithosphere, as shown schematically in figure 3(a). Recent work has shown that microplates may be driven by a drag imposed along their overlapping rifts in addition to the shear applied at their edges [22]. The stress fields resulting from the edge-driven and the rift-driven mechanisms, however, are indistinguishable [22] and thus the kinematics are independent of the partitioning of force between them.

We have derived a mathematical formulation of the Schouten model that we use to calculate the predicted shape of the inner pseudofaults for an image of a mature wax microplate (see appendix). The fit depends only on a single free parameter, the initial diameter of the microplate (defined below). All others are fixed or measured from observations of the conjugate outer

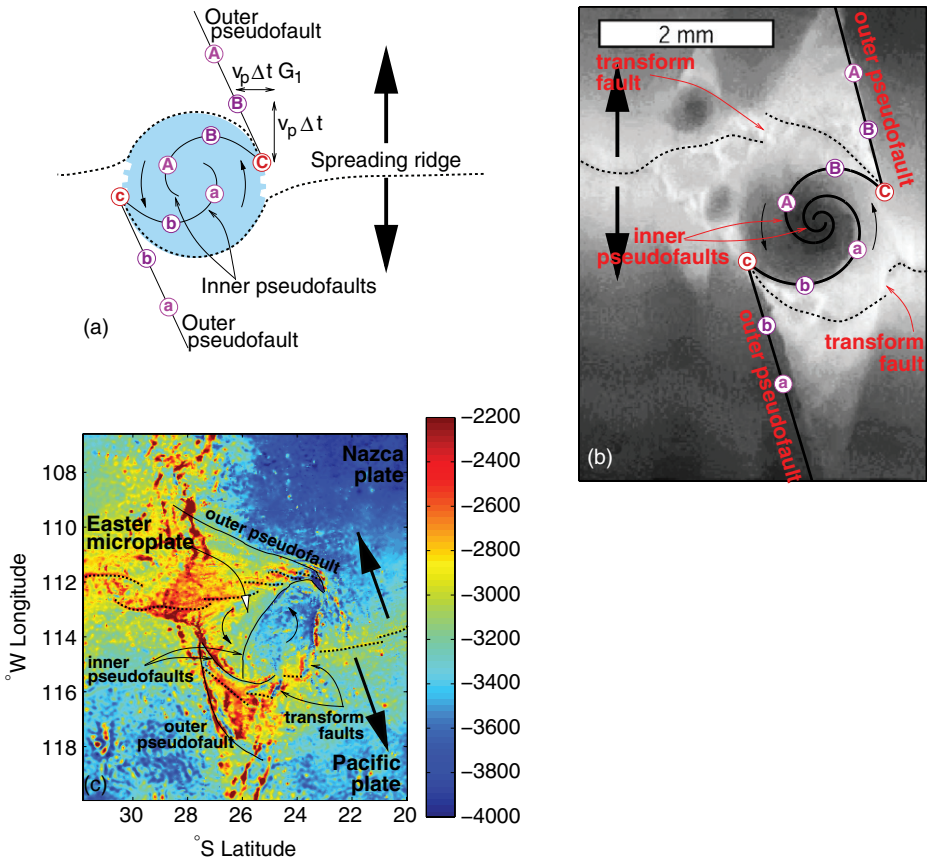

Figure 3. Three microplates: schematic, wax and Earth. Dashed lines show the position of the spreading rift. Solid lines mark the inner and outer pseudofaults. Large black arrows show the spreading direction. Small black arrows show the sense of microplate rotation. (a) Schematic diagram illustrating the kinematics of microplates according to the Schouten model. The letters indicate points on the pseudofaults that were formerly at the rift tips, showing how the microplate grows with time. The current positions of the rift tips are marked as (c) and (C). The linear outer pseudofaults indicate a constant radial growth rate, which in turn implies a logarithmic spiral inner pseudofault. (b) Image of a wax microplate with model fit and rift tip markers overlayed as in (a). Transform faults are labelled on the image. They are located laterally across the microplate from the rift tips. Note the brighter, thinner wax triangles above and below 'south' and 'north' of the microplate. The width of the thin-plate triangular region at any distance from the ridge shows the approximate diameter of the microplate at a time in the past. (c) Bathymetry of the Easter microplate [24]. Colours denote elevation with respect to sea level; the colour scale saturates at a minimum depth of 2200 m and a maximum depth of 4000 m. The Easter microplate is about 400 km across and is currently rotating clockwise at about 15° Ma^{-1}; over its lifetime of 5 Ma it has rotated about 95° [6]. Rift and pseudofault locations by D Naar, modified from Naar and Hey [14]. Note that this image has been rotated counterclockwise and reflected across the y-axis so that the orientation and sense of rotation of the microplate is consistent with panels (a) and (b).

pseudofaults and rift tip angles (defined below). Once one image has been fit, curves for the images of the microplate at earlier times are obtained by adjusting the time variable only. Figure 1 shows an example of the agreement of predicted with observed morphological time-evolution. Clearly, a similar time-series comparison for Earth is impossible; however, studies have compared predictions of the Schouten model with oceanic microplates and found reasonable agreement [5, 6]. We therefore conjecture, also based on the scaling analysis shown above, that wax microplates may be considered a laboratory analogue of those on the sea floor. We exploit this similarity to speculate on the nucleation of oceanic microplates based on our observations of wax. Other preliminary observations reveal intriguing correspondences between wax and Earth and underscore the potential power of our experimental approach.

4. Discussion

4.1. Nucleation of OSCs

Like oceanic microplates [25], wax microplates originate from OSCs which nucleate frequently on the spreading rift. Nucleation of wax OSCs occurs predominantly on ∼200–300 μm sections of obliquely spreading rift, where the rift normal is about 45° from the spreading direction. The diminished divergent component of spreading across these segments allows the rift axis to freeze across, introducing a discontinuity in the rift as shown in figure 4. This results in a local stress field tending to cause the propagation of rift tips into an overlapping geometry [26]–[28]. The rift tips will only propagate in this manner if the strength to tensile fracture of the adjacent lithosphere is small relative to the strength of the frozen rift. If, on the other hand, the adjacent lithosphere is too strong to be fractured by rift-tip propagation, deformation and faulting will remain localized on the rift centre. A muted strength contrast might be expected at fast spreading ridges where the adjacent lithosphere is thinner and weaker than at slow spreading ridges, consistent with the distribution of microplates on Earth. Furthermore, if applicable to Earth, this freezing-over mechanism of nucleation might explain the formation of OSCs on transform faults that have gained a component of divergence after a plate motion change or plate boundary re-organization [16, 17]. This reasoning equally applies to the wax, although we have not experimented with changes in spreading direction.

4.2. Relation to paleomicroplates

We observe a systematic relationship between on-axis, active microplates and their immediate predecessors that are being rafted away on one of the main plates. When the rift tip of a mature microplate reconnects to its opposing rift, it leaves an obliquely spreading segment which is unstable and rapidly converts to an OSC. This recurrence relation leads to ‘cascades’ of failed OSCs and microplates off-axis, an observation that is somewhat consistent with the paleoplates that are found off-axis on the ocean floor [29, 30].

4.3. Other similarities with Earth

Detailed observation of wax microplates reveals several interesting features. Figure 3(b) shows the location of transform faults associated with the microplate. The trace of these transform faults is evident in the triangle of contrasting brightness on the main plates ‘north’ and ‘south’ of the microplate. Brightness contrasts mark a discontinuity in plate age and thus in plate

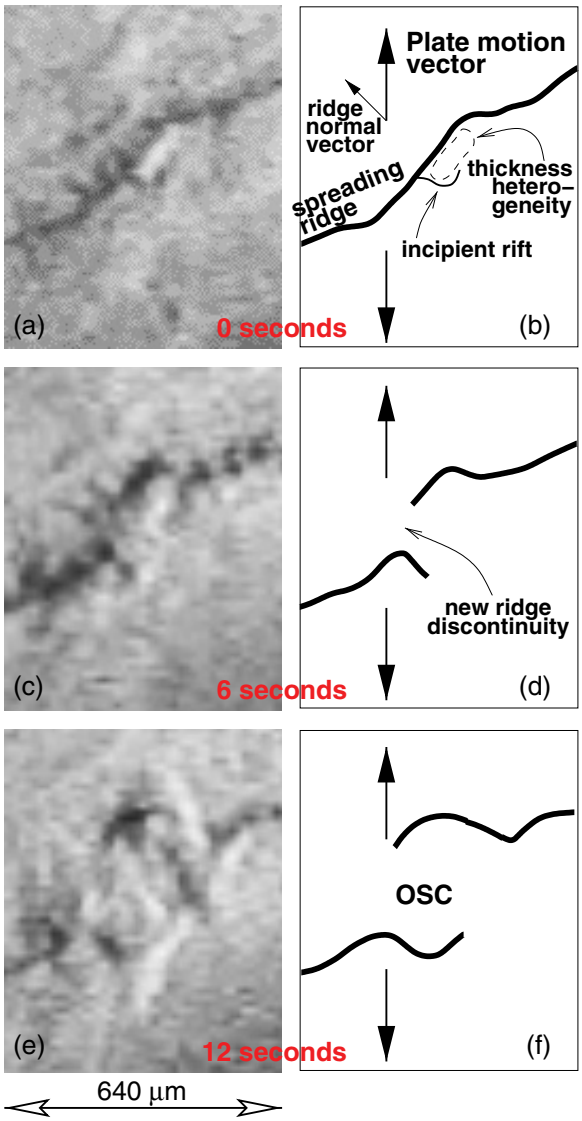

Figure 4. Nucleation of an OSC, precursor of a wax microplate. Left column, time series of images at high magnification. Right column, interpretive drawings mapping the evolution of the rift into an overlapping geometry. Note that interpretation is based on the movie from which these images were drawn. (a)–(b) Time $t = 0$ seconds. A section of rift with normal vector oriented 45° from the spreading direction. The OSC nucleates around a thickness heterogeneity at the rift which appears as an elongate white blob. (c)–(d) Time $t = 6$ seconds (∼1.2 Ma). A rift discontinuity appears and the disconnected rifts begin to overlap. (e)–(f) Time $t = 12$ seconds (∼2.4 Ma). Rifts are overlapping around an enclosed region with a diameter of about 300 μm. This OSC subsequently develops into a rotating microplate.

thickness. The brightness contrast on one side of the triangle marks the outer pseudofault, on the other side it results from the transform offset. We have also observed compression across the microplate margins between the rift tips and the spreading centre, evidenced by short wavelength

flexure of the microplate seen in figures 1(c) and (d). An analogous compressional zone has been inferred from sea-floor mapping and earthquake focal mechanisms associated with the Easter microplate [31, 33].

5. Conclusions

We have shown that a wax model of sea-floor spreading, under the right conditions, produces tectonic microplates that evolve in time according to a kinematic model designed for oceanic microplates. This finding suggests that wax microplates are a good analogue for microplates on the ocean floor and reinforces the validity of the kinematics prescribed by the Schouten model [6]. Furthermore, the presence of microplates in our analogue model indicates that, on Earth, microplates are a lithospheric phenomenon not dependent on special conditions or processes in the underlying mantle. Other similarities between wax and Earth noted here suggest that these models have potential to advance our understanding of microplates and other sea-floor spreading phenomena. For example, inferences drawn from repeated observation of the nucleation of wax microplates may apply to the birth of their oceanic counterparts. Establishment of dynamic scaling would permit quantitative predictions.

Acknowledgments

We thank D Naar and R Buck for comments and criticism that led to important changes in the manuscript. We also thank S Carbotte, D Bohnenstiehl, G Soffer, Z Karcz, W Pitman, M Spiegelman and one anonymous reviewer for their editorial suggestions. Discussions with S Tebbens led us to apply the Schouten model. Support for R Katz was provided by the Cornell Center for Material Research from the National Science Foundation Research Experience for Undergraduates program.

Appendix. Model formulation

In this section we derive a formulation of the model described by Schouten *et al* [6]. A schematic demonstration of the model is shown in figure 3(a). In general terms, we use measurements of the two outer pseudofaults to predict the spiral shape of their conjugate inner pseudofaults. To simplify the derivation and result, we assume that the growth rate of each spiral, $\mathrm{d}r_i/\mathrm{d}t$ is a constant, limiting the applicability of our formulation. The inner pseudofault radius as a function of time is

$$r_i(t) = v_p G_i t + R_0, \tag{A.1}$$

where v_p is the pulling rate (half spreading rate). Time, t, is zero when the incipient microplate becomes rigid and begins rotating. The initial radius, R_0 could be measured with higher resolution observations of incipient microplates. Our relatively crude images dictate that we consider R_0 to be a fit parameter. G_i is a geometric factor relating the rate of motion of the main plate to the lateral advance of a rift tip. i can take values 1 and 2 corresponding to each of the two pseudofault

pairs. From the geometry of the rift tip and outer pseudofault (figure 3(a)) G_i can be written as

$$G_i = \frac{\tan \alpha_i}{\cos \phi_i^f + \sin \phi_i^f \tan \alpha_i}, \tag{A.2}$$

where α_i is the outer pseudofault angle, the angle between the outer pseudofault and the spreading direction, and ϕ_i^f is the rift-tip angle, the angle formed by the perpendicular to the spreading direction and the line connecting the centre of the microplate and a rift tip. If $G_1 \neq G_2$ then the centre of the microplate will move with time. The radius of the entire microplate is

$$R(t) = v_p \frac{G_1 + G_2}{2} t + R_0. \tag{A.3}$$

The Schouten model states that the microplate is driven by a shear couple at its edges. Its angular velocity as a function of time, $\omega(t)$, is therefore given by the pulling rate divided by the radius of the microplate,

$$\omega(t) = \left(\frac{G_1 + G_2}{2} t + \frac{R_0}{v_p} \right)^{-1}. \tag{A.4}$$

Because it is easy to measure the final phase angle of the inner pseudofault (it is equal to the rift tip angle, ϕ_i^f) we integrate the angular velocity backward in time to give the phase angle as a function of time over the life of the microplate:

$$\phi_i(t) = \phi_i^f - \frac{2}{G_1 + G_2} \ln \frac{t + \psi}{t_f + \psi}, \qquad \psi = \frac{2R_0}{v_p(G_1 + G_2)}. \tag{A.5}$$

Using equations (A.1) and (A.5), we can write down a set of parametric equations for the inner pseudofault corresponding to the rift tip that we are considering:

$$x_i(t) = \pm(v_p G_i t + R_0) \cos \left[\phi_i^f - \frac{2}{G_1 + G_2} \ln \left(\frac{t + \psi}{t_f + \psi} \right) \right], \tag{A.6}$$

$$y_i(t) = \pm(v_p G_i t + R_0) \sin \left[\phi_i^f - \frac{2}{G_1 + G_2} \ln \left(\frac{t + \psi}{t_f + \psi} \right) \right], \tag{A.7}$$

where (x_i, y_i) is the position of the ith inner pseudofault as a function of time in the x–y coordinate system of the present time. Inner pseudofault trajectories drawn using equations (A.6) and (A.7) are overlayed on microplate images to visually test the goodness of fit, as in figure 1.

References

[1] Oldenburg D W and Brune J N 1972 Ridge transform fault spreading patterns in freezing wax *Science* **178** 301–4

[2] Oldenburg D W and Brune J N 1975 Explanation for the othogonality of ocean ridges and transform faults *J. Geophys. Res.* **80** 2575–85

[3] Bodenschatz E, Gemelke N, Carr J and Ragnarsson R 1997 Rifts in spreading wax layers: an analogy to the mid-ocean rift formation *Localization Phenomena and Dynamics of Brittle and Granular Systems* Columbia University

[4] Caress D W 1985 Some preliminary comments on parameter scaling in wax modeling, unpublished work

[5] Larson R L, Searle R C, Kleinrock M C, Schouten H, Bird R T, Naar D F, Rusby R I, Hooft E E and Lathiotakis H 1992 Roller-bearing tectonic evolution of the Juan Fernandez microplate *Nature* **356** 571–6
[6] Schouten H, Klitgord K D and Gallow D G 1993 Edge-driven microplate kinematics *J. Geophys. Res.* **98** 6689–701
[7] Herron E M 1972 Two small crustal plates in the South Pacific near Easter Island *Nature Phys. Sci.* **240** 35–7
[8] Forsyth D W 1972 Mechanisms of earthquakes and plate motions in East Pacific *Earth Plan. Sci. Lett.* **17** 189–93
[9] Anderson R N, Forsyth D W, Molnar P and Mammeric J 1974 Fault plane solutions of earthquakes on Nazca plate boundaries and Easter plate *Earth Plan. Sci. Lett.* **24** 188–202
[10] Hey R N 1977 A new class of pseudofaults and their bearing on plate tectonics *Earth Plan. Sci. Lett.* **37** 321–5
[11] Macdonald K C and Fox P J 1983 Overlapping spreading centres: new accretion geometry on the East Pacific Rise *Nature* **302** 55–8
[12] Macdonald K C, Scheirem D S and Carbotte S M 1991 Mid-ocean ridges: discontinuities, segments and giant cracks *Science* **253** 986–94
[13] Searle R C, Rusby R I, Engeln J, Hey R N, Zukin J, Hunter P M, LeBas T P, Hoffman H J and Livermore R 1989 Comprehensive sonar imaging of the Easter microplate *Nature* **341** 701–5
[14] Naar D F and Hey R N 1991 Tectonic evolution of the Easter microplate *J. Geophys. Res.* **96** 7961–93
[15] Macdonald K C, Fox P J, Perram L J, Eisen M F, Haymon R M, Miller S P, Carbotte S M, Cormier M H and Shor A N 1988 A new view of the mid-ocean ridge from the behavior of ridge-axis discontinuities *Nature* **355** 217–25
[16] Gallo D G and Fox P J 1982 Changes in relative plate motion: propagating ridges and the generation of oceanic micro-plates along accreting plate boundaries *EOS Trans. Amer. Geophys. Union* **63** 446
[17] Bird R T and Naar D F 1994 Intratransform origins of mid-ocean ridge microplates *Geology* **22** 987–90
[18] Obalth N S, Daniels K E, Bertsche W, Ragnarsson R and Bodenschatz E 2005 Parting the wax sea, in preparation
[19] Manga M and Sinton A 2004 Formation of bands, ridges and grooves on Europa by cyclic deformation: insights from analogue wax experiments *J. Geophys. Res.* **109** E09001
[20] Shell Synthetic Paraffin Waxes: Callista®wax *Technical report* Equilon Enterprises LLC 2001 www.shell-lubricants.com/Wax/pdf/ShellSyntheticParaffin.PDF
[21] Ragnarsson R, Ford J L, Santangelo C D and Bodenschatz E 1996 Rifts in spreading wax layers *Phys. Rev. Lett.* **76** 3456–9
[22] Neves M C, Searle R C and Bott M H P 2003 Easter microplate dynamics *J. Geophys. Res.* **108** 2213
[23] Turcotte D L and Schubert J 1982 *Geodynamics* (New York: Wiley)
[24] Smith W H F and Sandwell D T 1997 Global seafloor topography from satellite altimetry and ship depth soundings *Science* **277** 1957–62
[25] Hey R N, Johnson P D, Martinez F, Korenaga J, Somers M L, Huggett Q J, LeBas T P, Rusby R I and Naar D F 1995 Plate Boundary reorganization at a large-offset rapidly propagating rift *Nature* **378** 167–70
[26] De Bremaecker J C and Swenson D V 1990 Origin of overlapping spreading centers: a finite element study *Tectonics* **9** 505–19
[27] Grindley N R and Fox P J 1993 Lithospheric stresses associated with non-transform offsets of the Mid-Atlantic ridge: implications from a finite element analysis *Tectonics* **12** 982–1003
[28] Sempere J and Macdonald K C 1986 Overlapping spreading centers: implications from crack growth simulation by the displacement discontinuity method *Tectonics* **5** 151–63
[29] Mammerickx J and Naar D F and Tyce R L 1988 The mathematician paleoplate *J. Geophys. Res.* **93** 3025–40
[30] Bird R T, Tebbens S F, Kleinrock M C and Naar D F 1999 Episodic triple-junction migration by rift propagation and microplates *Geology* **27** 911–4
[31] Rusby R I and Searle R C 1993 Intraplate thrusting near the Easter microplate *Geology* **21** 311–4
[32] Naar D 2004 private communication
[33] Delouis B, Nicolas A, Ildefonse B and Philip H 1998 Earthquake focal mechanism and ocean thrust near Easter microplate: analogy with Oman ophiolite *Geophys. Res. Lett.* **25** 1443–6
[34] Dorset D L 2005 *Crystallography of the Polymethylene Chain: An Inquiry into the Structure of Waxes* (Oxford: Oxford University Press)